

Magnetic properties of YCo_5 compound at high pressure

E. Burzo,^{1,2} P. Vlaic,³ D. P. Kozlenko,⁴ N. O. Golosova,⁴
S. E. Kichanov,⁴ B. N. Savenko,⁴ A. Östlin,⁵ and L. Chioncel^{5,6}

¹*Faculty of Physics, Babes-Bolyai University 40084 Cluj-Napoca, Romania*

²*Romanian Academy of Science, Cluj-Napoca Branch, Cluj-Napoca 400015, Romania*

³*University of Medicine and Pharmacy Iuliu Hatieganu,*

Physics and Biophysics Department Cluj-Napoca, Romania

⁴*Frank Laboratory of Neutron Physics, Joint Institute for Nuclear Research, 141980 Dubna, Russia*

⁵*Theoretical Physics III, Center for Electronic Correlations and Magnetism,*

Institute of Physics, University of Augsburg, D-86135 Augsburg, Germany

⁶*Augsburg Center for Innovative Technologies (ACIT), D-86135 Augsburg, Germany*

(Dated: June 13, 2018)

The crystal structure and magnetic properties of YCo_5 compound have been studied by neutron diffraction, in the pressure range $0 \leq p \leq 7.2 \text{ GPa}$. The experimental data are analyzed together with results from the combined Density Functional and Dynamical Mean-Field Theory. A good agreement between the experimentally determined and calculated values of cobalt moments is shown. Our scenario for the behavior of YCo_5 under pressure, is the combined action of the Lifshitz transition with a strong local electron-electron interaction.

I. INTRODUCTION

The YCo_5 compound crystallize in the CaCu_5 -type structure, space group $P6/mmm$, with the cobalt atoms occupying $2c$ and $3g$ sites, while yttrium is located at the $1a$ site. The unit cell is formed of alternating $\text{YCo}(2c)/\text{Co}(3g)$ layers. The compound is ferromagnetic with cobalt moments of a dominant $3d$ -character. The magnetic moment at the $\text{Co}(2c)$ site is a little higher than that at the $\text{Co}(3g)$ site. Yttrium has an induced magnetic moment of $4d$ -band character which is significantly smaller and negatively polarized¹. First-principle, Density Functional Theory calculations were performed to investigate the pressure effects upon the crystal structure and magnetic properties of YCo_5 ²⁻⁴. The hallmark of the electronic structure in the YCo_5 compound is the presence of majority spin Co flat-bands of $3d$ -character, resulting from dispersion-less (localized) eigenstates along particular directions⁵ in the Brillouin zone. Upon pressure, electronic structure calculations predict a topological change in the band structure: the majority spin Co- $3d$ flat-band, located below E_F at ambient pressure, is shifted upwards in energy and leads to a structural instability when promoted above the Fermi level^{2,3}. This isomorphic structural transformation of YCo_5 was ascribed^{2,3} to a first order Lifshitz transition⁶. The corresponding threshold pressure for the electronically topological transition (ETT) to happen is predicted to be in the range of 10 – 20 GPa (Fig. 2, Ref. 2), depending on theoretical or experimental analysis^{2,3}. A transition from strong to weak ferromagnetism² was also associated with the ETT.

In this paper we report results of neutron diffraction (ND) measurements on YCo_5 compound, in the pressure range $0 \leq p \leq 7.2 \text{ GPa}$ and ambient temperature. To our best knowledge ND studies at higher pressures were not performed on YCo_5 nor are available in the literature. We supplement our experimental study, with re-

sults of electronic structure calculations using the combination of Density Functional⁷ and Dynamical Mean Field Theory^{8,9}, the LDA+DMFT^{10,11} method. At the standard DFT(LSDA) level we confirm the pressure dependent band structure calculations reported previously^{2,3}. Recent LDA+DMFT calculations for YCo_5 ¹² discussed the electronic correlations effects without pressure, in particular the formation and enhancement of orbital moments and magnetocrystalline anisotropy, as a function of electron-electron interaction parameters. In the current paper we follow the same methodology and complement this previous study, by discussing results for the band structures, density of states. The scenario we propose for the pressure dependence of the physical properties of YCo_5 takes into account the interplay between electronic correlations and Lifshitz transitions.

The paper is organized as follows: In Sec. II after a brief description of the experimental techniques the pressure dependence of neutron diffraction spectra, the changes in the unit cell parameters and magnetic moments is presented and analyzed. In Sec. III the experimental data is compared with the different models of the band structures obtained within DFT and its LDA+DMFT extension. Sec. IV presents a discussion and concludes our paper.

II. EXPERIMENTAL TECHNIQUES

The YCo_5 compound has been prepared by melting the high purity elements in an induction furnace, under high purity argon atmosphere. An excess of 2 % yttrium was used in order to compensate their loss during melting. The sample has been thermally treated at 1050 °C for 5 days. The X-ray diffraction pattern evidenced the presence of only one phase. The thermal variation of magnetization has been determined in the temperature range 4.2- 1000K and field up to 70 kOe.

Neutron diffraction measurements were performed in the pressure range $0 \leq p \leq 7.2 \text{ GPa}$, at $T = 290 \text{ K}$, with *DN-12* spectrometer¹³ at the *IBR-2* high flux pulsed reactor (FLNP JINR Dubna, Russia), using sapphire anvil high pressure cells¹⁴. The sample volume was about 4 mm^3 . Several tiny ruby chips were placed, at different points, on the sample surface. The pressure was determined by ruby fluorescence technique with the accuracy of 0.05 GPa , at each ruby chip and the pressure on the sample was obtained by averaging the values determined at different points. Diffraction patterns were collected at scattering angles 45.5° and 90° . The spectrometer resolution, at $\lambda = 2 \text{ \AA}$, is $\Delta d/d = 0.022$ and 0.015 for these angles, respectively. The typical data for collection time, at one temperature, was 20 hours.

A. Crystal and magnetic structures

The neutron patterns were analyzed by Rietveld method, using *MRIA*¹⁵ and *Full prof*¹⁶ programs. The errors in determining the cobalt moments, particularly in the high pressure range, are of $0.10 \mu_B$ - Table I. These are higher than the differences between magnetic moments at $2c$ and $3g$ sites¹. Consequently, even in the analysis of the high pressure data, the ordered magnetic moments of Co atoms at $2c$ and $3g$ sites, were assumed to be equal. The neutron diffraction patterns on YCo_5 compound, at $T = 290 \text{ K}$ and $p \leq 7.2 \text{ GPa}$, evidenced the presence of only one phase, having CaCu_5 -type structure - Fig. 1.

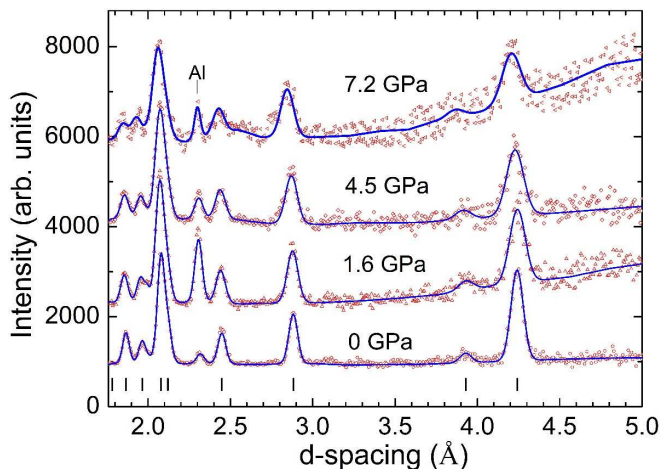


FIG. 1. Neutron diffraction patterns of YCo_5 at selected pressures, processed by the Rietveld method. The experimental points (red dots) and the calculated profiles (blue solid lines) are shown. The diffraction peaks include both nuclear and magnetic contributions and the ticks below the calculated profile indicate the position of the maxima. The position of extra peak from Al gasket of high pressure cell is also shown.

The a and c lattice parameters decrease with pressure, in an anisotropic way, see Fig. 2. The actual values of the unit cell parameters are provided in Tab. I.

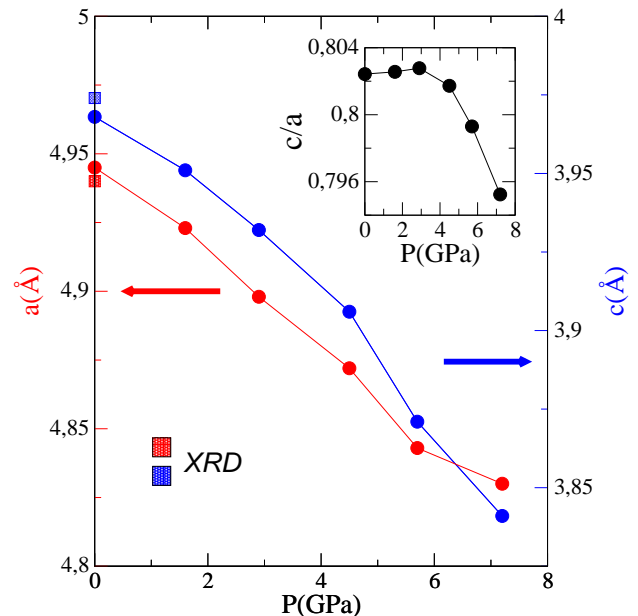


FIG. 2. The pressure dependences of lattice parameters, a (red circles) and c (blue circles). The variation of the c/a ratio as a function of pressure is shown in the inset. The blue/red boxes represent the c and a values obtained by XRD at room temperature and ambient pressure.

The c/a ratio (the inset of Fig. 2) increases slightly with pressure, reaches a maximum at about $p = 2.9 \text{ GPa}$ ($V/V_0 = 0.972$), then decreases further in value. At the maximum available pressure used in the present study ($p = 7.2 \text{ GPa}$) a volume reduction of $V/V_0 \approx 0.924$ is obtained. Note that the lattice parameters determined by XRD analysis at ambient conditions, are in excellent agreement with those obtained by neutron diffraction. At low temperatures the behavior of the c/a ratio, in the vicinity of the critical pressure allows to identify the nature of the transition as of first order². At $T = 100 \text{ K}$, there is a sharp decrease of the c/a ratio from 75.5 \AA^3 up to a minimum value at 74 \AA^3 ³³. At $T = 295 \text{ K}$, the decrease of this ratio is nearly linear and in an extended volume range, from 77.5 \AA^3 to 74 \AA^3 (Fig. 7, Ref. 3). This suggest a possible change of transition type.

The XRD studies under pressure in combination with density functional electronic structure calculations on YCo_5 compound suggested that an isomorphic structure transition takes place at $p = 19 \text{ GPa}$ at low temperature, while at room temperatures a similar transition happens for a pressure of 12 GPa ^{2,3}. Such a transition was described as a first order Lifshitz transition⁶.

The YCo_5 compound orders ferromagnetically¹. The thermal variation of magnetization at ambient pressure is given in Fig. 3. At $T = 4.24 \text{ K}$ the saturation magnetization is $7.7 \mu_B/f.u.$. In the temperature range $4.2\text{-}300 \text{ K}$, the magnetization decrease by 3% being of $7.42 \mu_B/f.u.$, at ambient condition, while the mean cobalt moment of

p (GPa)	0	1.6	2.9	4.5	5.7	7.2
a (Å)	4.945(3)	4.923(7)	4.898(9)	4.872(9)	4.843(9)	4.830(9)
c (Å)	3.968(4)	3.951(8)	3.932(8)	3.906(8)	3.871(9)	3.841(9)
Mean Co moment	1.48(9)	1.36(10)	1.35(10)	1.29(10)	1.24(10)	1.05(10)

TABLE I. Measured pressure-dependent lattice parameters and mean cobalt moments.

$1.48 \mu_B/\text{atom}$ remains nearly the same. In order to compare the evolution with pressure of total moments, the experimentally determined values, at $T = 290$ K, were extrapolated to $T = 0$ K, according to $T^{3/2}$ law, which describes also the temperature dependence of YCo_5 magnetization, at $T/T_c \leq 0.3$ - Fig. 3. The extrapolated cobalt moments, are only by $0.04 \mu_B$ higher than those determined at $T = 290$ K. Finally, the measured and computed (DMFT) total moments agree rather well, see Fig. 3. In addition we compare in Fig. 3 our results also with the recent experiments, of Ref. 17, on single crystals. The DMFT results show a rather uniform temperature dependence in the range of 200 to 600 K. The fitting of the experimental data with a $\sqrt{1 - T/T_c}$ dependence in the temperature range of 800 to 1000 K, leads to a value $T_c \approx 975$ K, which is in the range of experimental values discussed in the review paper Ref. 18.

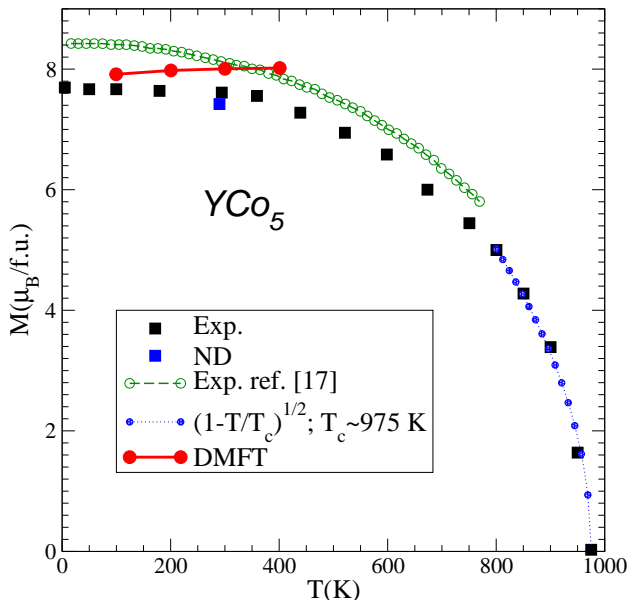


FIG. 3. Temperature dependence of spontaneous magnetization at ambient pressure. Computed data: Red solid line - DMFT. The last few points of the neutron diffraction data (black squares) were fitted with $\sqrt{1 - T/T_c}$ (blue circles). Single-crystal experiments of Ref. 17, green circles. Difference between single-crystal data (green circles) and powder sample (black squares) are consistent with previous findings¹⁹.

The relatively large orbital moments²⁰ of Co couple to the spin moments (spin-orbit coupling) and establish the direction of cobalt spin moments along the crystallographic axes. The local anisotropy (stabilization energy)

was experimentally estimated at $2.88 \cdot 10^{-4}$ erg/atom for $\text{Co}(2c)$ sites and a smaller but opposite contribution $-0.84 \cdot 10^{-4}$ erg/atom arises from the $\text{Co}(3g)$ sites^{21,22}. The anisotropy energy, can also be computed using the density functional theory²³⁻²⁸. Its magnitude was found to be strongly affected by changes of the lattice geometry (c/a ratio and volume)²⁸, and by the degree of filling of $\text{Co-}3d$ bands. In particular for the band filling corresponding to a mean cobalt moment of $0.6 \mu_B$, an easy plane of magnetization was shown to be favored²⁸.

The cobalt moments, M_{Co} , as function of pressure p , are given in Tab. I. As can be seen, the cobalt moments change little with pressure. For a decrease in relative volume up to $V/V_0 \approx 0.92$, the changes were interpreted as a consequence of a high-spin to low-spin state transition^{2,3} with a larger decrease for the cobalt moments at the $3g$ position. This behavior was also connected with the different local environments of $\text{Co}(2c)$ and $\text{Co}(3g)$ sites. By further increasing pressure, up to a relative volume $V/V_0 = 0.8$ the cobalt moments collapse as previously obtained by full potential density functional calculations^{2,3}. Along with the high-spin to low-spin transition, the spin reorientation transition (frequently present in the family or RCO_5 compounds²³⁻²⁸) may also take place and contribute to the moment reduction. In addition we observe that the combined structural and magnetic transformation resembles the situation already pointed out for the GdCo_5 compound⁴. In the ferromagnetic GdCo_5 the magnetic interaction paths follow the Campbell model²⁹ and because the $\text{Gd}(4f)$ -states are situated away from the Fermi level, at the Fermi surface the bands have a dominant $\text{Co}(3d)$ -states character. Having the same crystal structure dispersion-less $\text{Co}(3d)$ -bands are expected to be seen in the band structure³⁰ of GdCo_5 . Therefore, we *predict* that under pressure GdCo_5 may also show signatures of a possible Lifshitz transition, unnoticed previously because of the focus on the strong magnetism of $4f$ states.

III. DENSITY FUNCTIONAL THEORY CALCULATIONS

In the present paper the full-potential linearized muffin-tin orbitals (FPLMTO) method, as implemented in the RSPT code^{31,32}, was employed. The calculations have been performed using the LDA with the parametrization of Perdew and Wang³³ for the exchange-correlation functional. Three kinetic energy tails were used, with corresponding energies 0.3, -2.3 , and -1.5

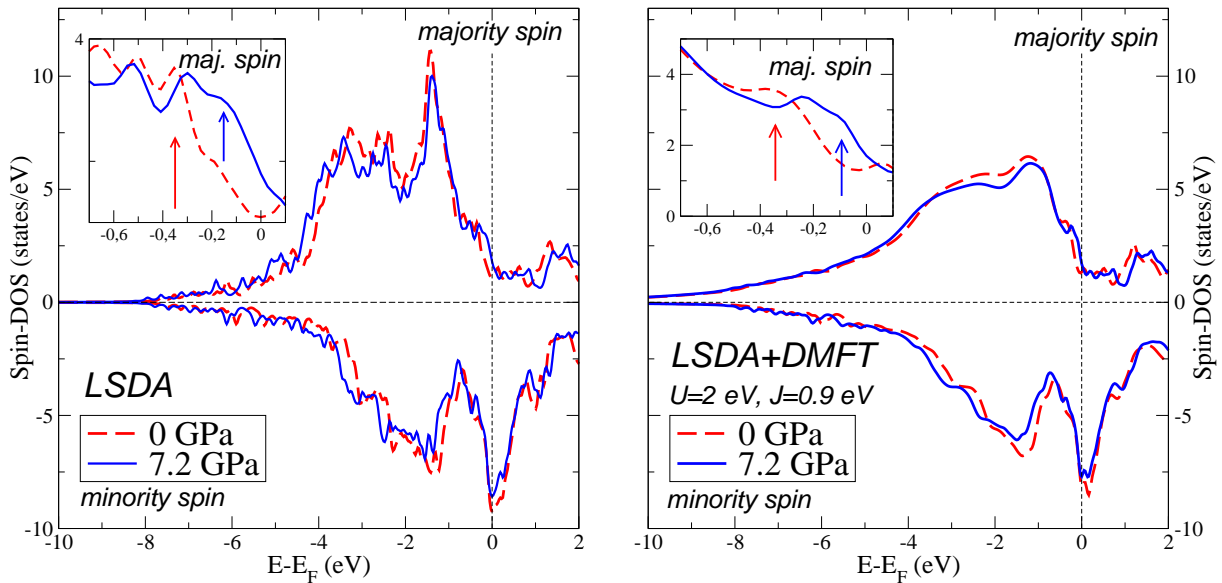


FIG. 4. Spin-resolved total densities of states for LSDA (left) and LSDA+DMFT (right). Ambient pressure and $p = 7.2$ GPa is denoted by red dashed lines and blue solid lines, respectively. Arrows in the insets indicate the change in the position of flat bands.

Ry. The \mathbf{k} -mesh grid was $6 \times 6 \times 6$, and a Fermi-Dirac smearing with $T = 474$ K was used. The muffin-tin radius was set to 2.1 a.u. for the Co atoms, and to 2.3 a.u. for the Y atom, and was kept constant for all pressures. The calculations included spin-orbit coupling and scalar-relativistic terms. A very important property of YCo_5 is the magnetocrystalline anisotropy which derives from the large orbital magnetic moments on Co observed in experiment^{22,34,35}. In order to capture the large orbital polarization (OP), non-ab-initio DFT+OP has been previously employed^{36,37}. The physical origin of the proposed OP corrections derives from the atomic limit. Alternatives to this method are the relativistic implementation of the LDA+U or the more recently developed LDA+DMFT. In both these techniques a multi-orbital Hubbard term is added to the DFT, and the “upgraded” Hamiltonian is solved either by a static mean field decoupling (+U), or by using a full many-body approach (DMFT). The Hubbard terms are constructed from a set of Coulomb U and exchange J parameters. We have performed in this paper LDA+DMFT calculations within the FPLMTO method. For the DMFT scheme, the perturbative spin polarized T -matrix fluctuation-exchange (SPT-FLEX) impurity solver has been used³⁸. The solver is implemented on the imaginary-axis Matsubara domain, and the temperature was set equal to that used for the Fermi-Dirac smearing. We consider Hubbard corrections only to the Co- $3d$ orbitals, set $J = 0.9$ eV, while allowing U to vary in the range of 1.0 eV to 3.0 eV.

A. Density of States and Band Structures

In all calculations we include the SO coupling and take the magnetization oriented along the c -axis. Nevertheless, we have checked that for the cases in which the moment is oriented within the (ab) -plane the $3g$ sites splits into two inequivalent sites, one of multiplicity one and the other with multiplicity two.

In Fig. 4 we show the total spin-resolved density of states using the LSDA (left panel) and including the DMFT correction (right panel). For both LSDA(+DMFT) density of states the majority spin channel (\uparrow) is almost complete, while the Fermi level in the minority spin (\downarrow) is pinned around a maximum. The orbital contribution to the maximum in the minority spin DOS has a predominant $d_{x^2-y^2}/d_{xy}$ -character. Both Co($2c$)/(3 g)-sites contribute, however Co($2c$)-sites have a stronger weight around E_F . Correlation induced modification in DOS (seen in Fig. 4) are: (i) a broadening of the spectra because of the presence of many-body self-energy $\Sigma(E)$, and (ii) the appearance of tails in the density of states at higher binding energies. These changes are similar for the ambient pressure ($V/V_0 = 1.0$) as well as for the $p = 7.2$ GPa ($V/V_0 = 0.924$). The insets of Fig.4 present the majority spin-channels (\uparrow), with the arrows pointing to the energies at which the dispersion-less bands are obtained.

The band structure including the SO coupling is presented in Fig 5. At ambient pressure (left panel Fig. 5) the dispersion less band indicated within the blue box is located at about -0.3eV below E_F . Upon pressure (right

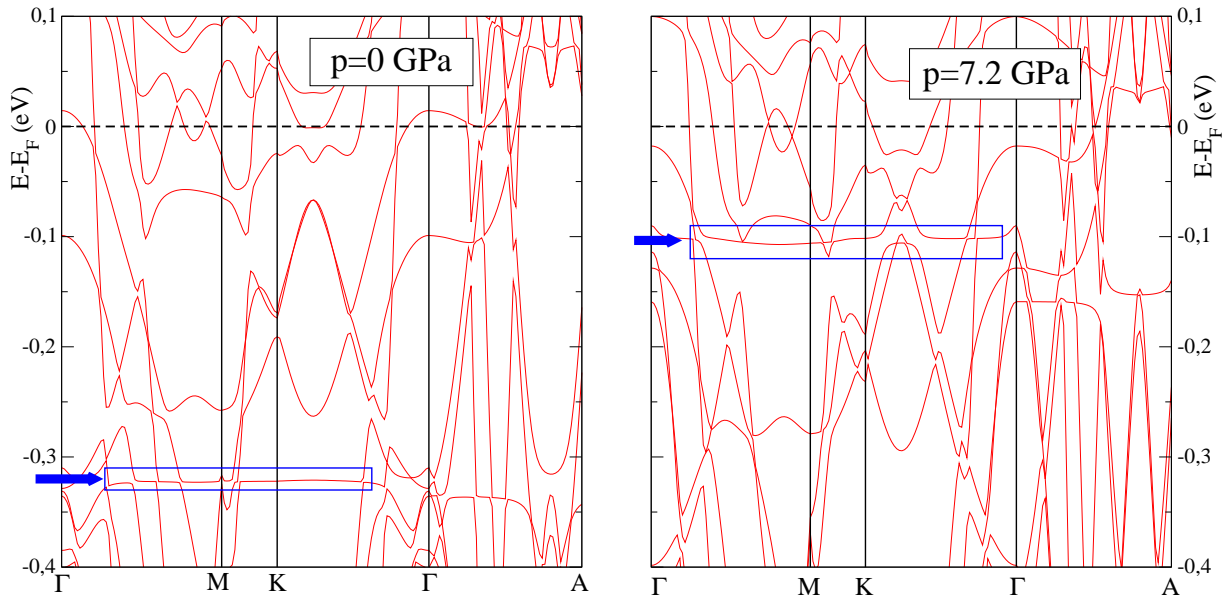


FIG. 5. Band structure for ambient pressure (left) and $p = 7.2$ GPa (right) computed within the LSDA including the spin-orbit coupling. Computed moments are oriented along the z -direction. Blue boxes and arrows indicate the position of flat bands.

panel Fig. 5) the flat band approaches the Fermi level and in the same time a slight departure from the flatness is seen. In the absence of spin-orbit coupling we have checked that these flat bands reveal their d_{yz}/d_{zx} -orbital character in agreement with the previous results^{2,3}. The first order Lifshitz transition was associated with the shifting of the dispersion-less band as pressure is increased^{2,3}, however electronic correlations were ignored.

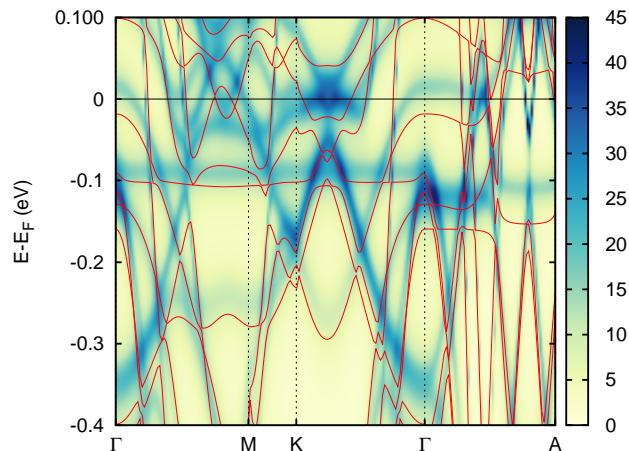


FIG. 6. LDA+DMFT Bloch spectral function at 7.2 GPa, using $U = 2$ eV and $J = 0.9$ eV. Red lines correspond to the LSDA band structure.

In Fig. 6 we compare the LDA band structure of Fig. 5 corresponding to the pressure of 7.2 GPa with the LDA+DMFT spectral function. Of interest are the

bands situated with 0.1 eV below E_F where the LDA predict, under pressure, a shifted flat band. This band is further pushed towards E_F as a consequence of the negative slope of the real-part of the self-energy, however there is no significant change in its flatness. Therefore electronic correlations and pressure have the same effect in bringing the flat-band closer to E_F . Consequently, the LDA based prediction for the threshold pressure for the Lifshitz transition may be decreased because of the presence of electronic correlations. Further investigations are necessary for a quantitative prediction of the threshold value which goes beyond the scope of the present study. A more detailed discussion on the combined effect of correlation and Lifshitz transition is presented in Sec. IV.

B. Magnetic moments and orbital polarizations

Our results for the spin μ_s and orbital μ_l moments at Co(2c)/Co(3g) sites are $\mu_s = 1.53/1.54\mu_B$ and $\mu_l = 0.22/0.18\mu_B$ at ambient pressure and $\mu_s = 1.45/1.45\mu_B$ and $\mu_l = 0.18/0.15\mu_B$ at 7.2 GPa respectively. These results can be compared with the experimental values given by ND experiment, see Sec. II. In the neutron diffraction experiment the spin and orbital scattering form factors are not separated, nor site resolved, we consider to average the computed moments according to their different environments, which is sensitive to different pressures. The experimentally determined pressure/relative volume dependence of cobalt moments is in rather good agreement with the theoretical data in particular at $V/V_0 > 0.93$. The decrease of cobalt moments

was previously studied theoretically within the rigid band model^{23–25,28}. More recently, this decrease was associated with a high to a low spin state transition that takes place at $V/V_0 \approx 0.92$, simultaneously with the isomorphic structural change^{2,3}.

There have been numerous theoretical works on the magnetocrystalline anisotropies (MAE) of YCo_5 ^{12,24,25,28,36,39}. The MAE values originate from the large orbital magnetic moments of Co atoms with a slightly larger contribution originating from the 2c sites.

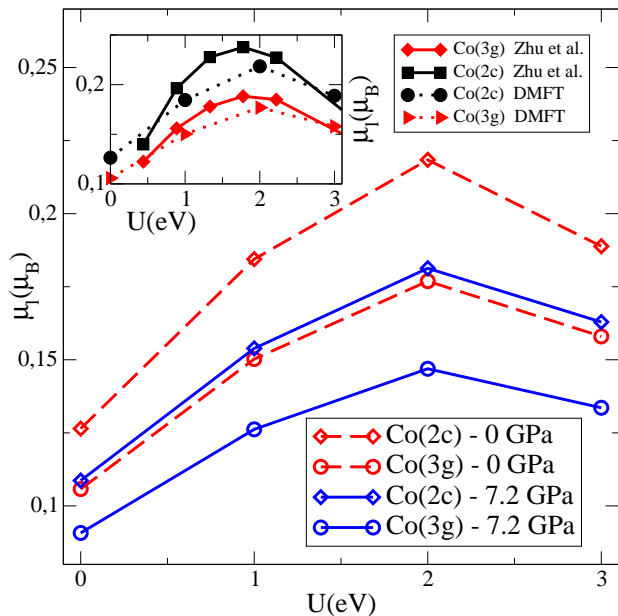


FIG. 7. Orbital magnetic moments of Co(2c)/(3g) atom at ambient pressure (red dashed) and at 7.2 GPa (blue solid) as a function of the Coulomb parameter U , for fixed $J = 0.9$ eV. Inset: Ambient pressure results in comparison with Ref. 12.

In Fig. 7 we present the LDA+DMFT results for the computed orbital moments as function of the strength of local Coulomb interaction U and for a fixed value of the exchange parameter J . We preliminary checked that changes in the orbital moment are very small with respect to J , so we varied U within the reasonable range of values for transition metal elements, while keeping $J = 0.9$ eV fixed. The atom resolved Co(2c) and Co(3g) orbital moments reach maximum values for U about 2 eV. Our results for the orbital moments are consistent with previous X-ray magnetic circular experiments¹², inelastic spin flip neutron scattering experiments⁴⁰ and calculations including the orbital polarization scheme^{24,28} or the recent LDA+DMFT¹².

The magnetic properties of Y are induced by the hybridization with neighboring Co atoms in the basal-(ab) plane. We observe that upon increasing pressure the $\text{Y}4d\text{-Co}3d$ hybridization and consequently the negative polarization induced on $\text{Y}4d$ bands increases. Its magnitude which we denote by M_{4d} , depends on the number

of cobalt atoms situated in the first coordination shell to an Y atom (z_i) and their magnetic moments $M_{\text{Co}i}$. Note that for YCo_5 the ratio $|M_{4d}|/\sum_i z_i M_{\text{Co}i} = 1.2 \cdot 10^{-2}$ has nearly the same value as evidenced in RM_5 compounds (where $M = \text{Co}, \text{Ni}$ and $R = \text{heavy rare-earth}$), for which a value $1.3 \cdot 10^{-2}$ was obtained⁴¹. Therefore the d-bands of the transition metal elements not only mediate the dominant $4f$ -magnetism of heavy rare-earths in the RM_5 compounds, but also polarize the $\text{R}5d$ band of rare-earth atoms. Our estimation for the ratio $|M_{4d}|/\sum_i z_i M_{\text{Co}i}$ in YCo_5 , show that also in the absence of dominant $4f$ -magnetism this effect is still present, with a similar intensity.

IV. DISCUSSIONS AND CONCLUSION

According to Koudela *et al.*³, the first order structural transition under pressure can be ascribed to a Lifshitz transition. However, in this scenario the many-body electronic correlation effects are completely disregarded. On the other hand electronic correlations are essential to capture the considerable orbital polarization in this compound. A specific question which appears is the interplay of the electronic correlation and the Lifshitz transition. In this section we discuss the behavior of the flat-band (related to the Lifshitz transition) and the energy dependence of the imaginary part of the self-energy (related to many-body effects) of YCo_5 under pressure.

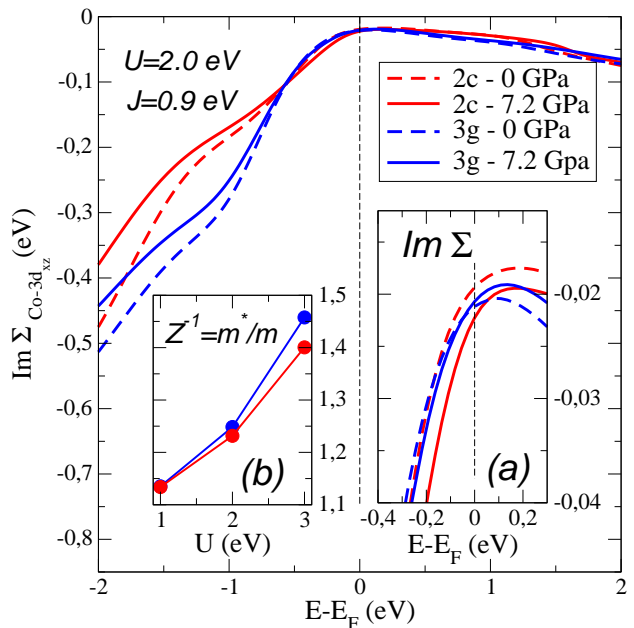


FIG. 8. Self-energies for the d_{xz} -orbital at ambient pressure (dashed) and at $p = 7.2$ GPa (solid), for Co atoms at (2c/3g) site with red/blue lines. Inset (a) a reduced energy window around E_F . Inset (b) Effective mass renormalization as function of U at ambient pressure.

In Fig. 8 we show the imaginary part of the self-energy for the Co(2c) and Co(3g) atoms for the selected d_{xz} orbital contributing to the flat bands. All the other orbitals have a qualitatively similar energy-dependence of the imaginary part of the self-energy. The results for the ambient pressure are presented with dashed lines, while continuous lines are used for the results at 7.2 GPa. The right inset presents the $Im \Sigma_{xz}(E)$ in the energy window $[-0.4eV, 0.3eV]$ around E_F . At ambient pressure, the dispersion-less band is situated at larger distance from E_F , therefore the system is away from the Lifshitz transition. The self-energy follow the Fermi-liquid behavior, i.e. a parabolic energy dependence $Im \Sigma_{xz}(E) \propto (E - E_F)^2$. At 7.2 GPa the flat-band approaches the Fermi level and a slight departure from the flatness can be seen (Fig. 5). Electronic correlations push the dispersion less band even closer to the E_F .

Local on-site correlation effects are dominant in the scattering rates related to electron-electron interaction and can be studied in the framework of LDA+DMFT. The quasiparticle scattering rate Γ_{ee} of the charge carriers can be computed from the imaginary part of the self-energy, according to the formula: $\Gamma_{ee} = Z \cdot Im\Sigma_{xz}(E)$, where $Z^{-1} = (m^*/m_{LDA})$ is the renormalization factor which in case of electronic correlations reduces the step of momentum density at k_F . In the left inset of Fig. 8 the results for the mass enhancement as a function of the strength of Coulomb interaction U is presented. This is computed from the self-energy according to: $m^*/m_{LDA} = [1 - \partial Im\Sigma/\partial\omega_n|_{i\omega_n \rightarrow 0}]^{-1}$. The effective mass monotonically increases with U similar to

the previous results¹², implying a monotonic decrease of Z . This term contributes as a multiplicative constant to the $\Sigma_{xz}(E)$ consequently, the scattering rate follows also a Fermi-liquid behavior. Resistivity under pressure was shown to follow a similar behavior in RCo₅-compounds⁴².

In summary, the present paper discusses the properties of YCo₅ near a structural transition induced by pressure. Our neutron diffraction experiment and the corresponding theoretical modeling within LDA+DMFT, is performed up to a pressure of 7.2 GPa. Although at this pressure the system does not reach the possible Lifshitz transition proposed previously^{2,3}, we study the behavior of the bands, density of states and magnetic moments. Our many-body calculations reveal that the imaginary part of the self-energy follows a parabolic energy dependence approaching the Lifshitz transition. However, for stronger Coulomb U parameters the slope of the real part of the self-energy increases, and accelerate the proximity to the Lifshitz transition. The increase in the effective mass acts as a multiplicative constant to the imaginary part of the self-energy, therefore the scattering rate would also follow the Fermi-liquid behavior. Finally, according to our results the physical properties of YCo₅ under pressure could be described supplementing the Lifshitz scenario^{2,3,30} with strong local electron-electron interaction.

ACKNOWLEDGMENT

A.Ö and L.C. acknowledges financial support offered by the Augsburg Center for Innovative Technologies, and by the Deutsche Forschungsgemeinschaft (through the project TRR 80/F6).

-
- ¹ E. Burzo, A. Chelkowski, and H. R. Kirchmayr, in *Landolt Börnstein Handbook*, Vol. 19d2 (Springer Verlag, Heidelberg, 1990) p. 130.
- ² H. Rosner, D. Koudela, U. Schwarz, A. Handstein, M. Hanfland, I. Opahle, K. Koepnik, M. D. Kuz'min, K. H. Müller, J. A. Mydosh, and M. Richter, *Nature Physics* **2**, 469 (2006).
- ³ D. Koudela, U. Schwarz, H. Rosner, U. Burkhardt, A. Handstein, M. Hanfland, M. D. Kuz'min, I. Opahle, K. Koepnik, K.-H. Müller, and M. Richter, *Phys. Rev. B* **77**, 024411 (2008).
- ⁴ E. Burzo and P. Vlaic, *AIP Conf. Proc.* **1564**, 103 (2013).
- ⁵ M. Ochi, R. Arita, M. Matsumoto, H. Kino, and T. Miyake, *Phys. Rev. B* **91**, 165137 (2015).
- ⁶ I. M. Lifshitz, *Sov. Phys. JETP* **11**, 1130 (1960).
- ⁷ W. Kohn, *Rev. Mod. Phys.* **71**, 1253 (1999).
- ⁸ W. Metzner and D. Vollhardt, *Phys. Rev. Lett.* **62**, 324 (1989).
- ⁹ G. Kotliar and D. Vollhardt, *Physics Today* **57**, 53 (2004).
- ¹⁰ G. Kotliar, S. Y. Savrasov, K. Haule, V. S. Oudovenko, O. Parcollet, and C. A. Marianetti, *Rev. Mod. Phys.* **78**, 865 (2006).
- ¹¹ K. Held, *Adv. Phys.* **56**, 829 (2007).
- ¹² J.-X. Zhu, M. Janoschek, R. Rosenberg, F. Ronning, J. D. Thompson, M. A. Torrez, E. D. Bauer, and C. D. Batista, *Phys. Rev. X* **4**, 021027 (2014).
- ¹³ V. Aksenov, A. Balagurov, V. Glazkov, D. Kozlenko, I. Naumov, B. Savenko, D. Sheptyakov, V. Somenkov, A. Bulkin, V. Kudryashev, and V. Trounov, *Physica B* **265**, 258 (1999).
- ¹⁴ V. P. Glazkov and L. Goncharenko, *Fiz. Tekh. Vys. Davlenii* **1**, 56 (1991).
- ¹⁵ V. B. Zlokazov and V. U. Chernyshev, *J. Appl. Crystallogr.* **25**, 447 (1992).
- ¹⁶ J. Rodriguez-Carvajal, *Physica B* **192**, 55 (1993).
- ¹⁷ C. E. Patrick, S. Kumar, G. Balakrishnan, R. S. Edwards, M. R. Lees, E. Mendive-Tapia, L. Petit, and J. B. Staunton, *Phys. Rev. Materials* **1**, 024411 (2017).
- ¹⁸ K. H. J. Buschow, *Rep. Prog. Phys.* **40**, 1179 (1977).
- ¹⁹ G. H. O. Daalderop, P. J. Kelly, and M. F. H. Schuurmans, *Phys. Rev. B* **53**, 14415 (1996).
- ²⁰ J. Deportes, D. Givord, J. Schweizer, and F. Tasset, *IEEE Trans. Magn. MAG* **12**, 1000 (1976).
- ²¹ R. L. Streever, *Phys. Letters* **63A**, 360 (1978).
- ²² R. L. Streever, *Phys. Rev. B* **19**, 2704 (1979).
- ²³ G. H. O. Daalderop, P. J. Kelly, and M. F. H. Schuurmans, *Phys. Rev. B* **44**, 12054 (1991).
- ²⁴ L. Nordström, M. S. S. Brooks, and B. Johansson, *J. Phys: Condens. Matter* **4**, 3261 (1992).

- ²⁵ M. Yamaguchi and S. Asano, J. Appl. Phys. **79**, 5952 (1996).
- ²⁶ H. J. F. Jansen, Phys. Rev. B **59**, 4699 (1999).
- ²⁷ H. Yamada, K. Terao, F. Ishikawa, M. Yamaguchi, M. Mitamura, and T. Goto, J. Phys: Condens. Matter **11**, 483 (1991).
- ²⁸ L. Steinbeck, M. Richter, and H. Eschrig, Phys. Rev. B **63**, 184431 (2001).
- ²⁹ I. A. Campbell, J. Phys. F: Metal Phys. **2**, L47 (1972).
- ³⁰ M. Ochi, R. Arita, M. Matsumoto, H. Kino, and T. Miyake, Phys. Rev. B **91**, 165137 (2015).
- ³¹ J. M. Wills, M. Alouani, P. Andersson, A. Delin, O. Eriksson, and O. Grechnev, *Full-Potential Electronic Structure Method* (Springer, Berlin, 2010).
- ³² O. Grånäs, I. D. Marco, P. Thunström, L. Nordström, O. Eriksson, T. Björkman, and J. Wills, Comp. Mater. Sci. **55**, 295302 (2012).
- ³³ J. P. Perdew and Y. Wang, Phys. Rev. B **45**, 13244 (1992).
- ³⁴ J. Schweizer and F. Tasset, J. Phys. F **10**, 2799 (1980).
- ³⁵ J. M. Alameda, D. Givord, R. Lemaire, and Q. Lu, J. Appl. Phys. **52**, 2079 (1981).
- ³⁶ L. Nordström, O. Eriksson, M. S. S. Brooks, and B. Johansson, Phys. Rev. B **41**, 9111 (1990).
- ³⁷ P. S. B. S. M. D. L. X. Benedict, D. Aberg, LLNL-TR-678582 (2015).
- ³⁸ A. I. Lichtenstein and M. I. Katsnelson, Phys. Rev. B **57**, 6884 (1998).
- ³⁹ P. Larson, I. I. Mazin, and D. A. Papaconstantopoulos, Phys. Rev. B **67**, 214405 (2003).
- ⁴⁰ A. Heidemann, D. Richter, and K. H. J. Buschow, Zeitschrift Für Phys. B Condens. Matter **22**, 367 (1975).
- ⁴¹ E. Burzo, L. Chioncel, R. Tetean, and O. Isnard, J. Phys: Condens. Matter **23**, 026001 (2011).
- ⁴² N. Hong, R. Hauser, G. Hilscher, E. Gratz, R. Ballou, and H. Ido, Journal of Magnetism and Magnetic Materials **140-144**, 933934 (1995).